Journal of Applied Science and Engineering, Vol. 20, No. 2, pp. 193–200 (2017) *DOI: 10.6180/jase.2017.20.2.07*

A Novel Color Image Watermarking Scheme Based on DWT and QR Decomposition

Shaoli Jia*, Qingpo Zhou and Hong Zhou

School of Civil Engineering, Ludong University, Yantai 264025, P.R. China

Abstract

A novel color image watermarking scheme based on DWT (Discrete Wavelet Transform) and QR decomposition is proposed to embed color watermark image into color host image. Firstly, the each component of the color host image is transformed by one-level DWT, and further divided to 4×4 non-overlapping pixel blocks. Then, each selected pixel block is decomposed by QR decomposition and the first row elements in the matrix R is quantified for embedding the watermark information. In the extraction procedure, the watermark can be extracted from the watermarked image without the requirement of the original host image or the original watermark image. Experimental results, compared with the related existing methods, show that the proposed color image scheme has stronger robustness against most common attacks such as image compression, filtering, cropping, noise adding etc.

Key Words: Color Image Watermark, Discrete Wavelet Transform, QR Decomposition, Blind Extraction

1. Introduction

With the rapid development of Internet and multimedia technology, how to protect the copyright of products from the illegal usage has been receiving more and more attention. Among the published techniques of copyright protection, digital watermarking is considered as a powerful method [1,2]. The feature of digital watermarking is to allow for imperceptibly embedding watermark information in the original multimedia data. In the past decades, many digital watermarking techniques have been developed.

In recent years, color image watermarking has been becoming one of the hot research topics [3]. Compared with gray-level image, the color one has two advantages: (1) can hide a greater amount of data; (2) can attain higher fidelity, which is because the color perception depends not only on the luminance but also on the chrominance. Thus, by using color image watermarking scheme, both the capacity and the fidelity can be improved.

The Discrete Wavelet Transform (DWT), as an important mathematic method, has extensively been used for watermarking color images [4]. The main advantage of using DWT for robust watermarking schemes is that it better takes into account the local image characteristics at different resolution levels which can significantly improve the robustness and invisibility of the watermark. By adopting a frequency spread of the watermark together with a spatial localization, these schemes are able to better conceal the watermark within the salient components of the image. Each level of the DWT decomposition generates four bands denoted by LL, HL, LH, and HH. The LL sub-band is further decomposed to obtain another level of decomposition. This procedure continues until the desired number of decomposition levels is reached. The LL sub-band represents the information at all coarser scales. Generally, a pseudo-random number (PRN) sequence is embedded in a selected set of the DWT coefficients and the strength of the embedded watermark is adjusted with the help of scaling factors for

*Corresponding author. E-mail: ldustudy@163.com

each band. For example, in [4] the authors proposed to compute the local entropies of the image wavelet coefficients to control the imperceptibility and to achieve an enhanced detection and localization of the watermark.

Among the existing dual color image watermarking schemes, a blind color image watermarking was proposed in [5], one or more singular values must be modified to keep the order of singular values, which might degrade the quality of the watermarked image. In addition, the SVD has higher computational complexity. Especially, when the problem is of recursive nature, the SVD requires $O(n^3)$ flops for a matrix of order n. As a major intermediate step in SVD, QR decomposition has lower computational complexity than SVD since the former only needs $O(n^2)$ flops while the latter needs $O(n^3)$ [6,7]. The feature highlights the use of QR decomposition in digital watermarking and some methods have been proposed in [8–10]. Yashar et al. [8] proposed to embed a watermark bit in all elements of the first row of R matrix after each 8×8 block was decomposed by QR decomposition, in which the watermark was 88×88 binary image. In [9], a 32×32 binary image was embedded into the 512×512 host image by modifying the elements in the Q matrix. The method [8] or [9] could not be better used to embed large amounts of color watermark information into host image since the binary image was used as the original watermark in [8] or [9]. In [10], only the first row forth column $r_{1,4}$ of R matrix can be quantified for embedding watermark when performing QR decomposition on 4×4 pixels matrix, which limits the capacity of the watermark. Theoretically, all elements in the first row of R matrix can be used to embed watermark when only use QR decomposition to the original block, that is, its capacity can be 0.125 (bits/pixel). In addition, the MD5-based Hash pseudo-random replacement algorithm with private key K_i (i = 1, 2, 3) is used to select the embedding block for embedding watermark in [10], which will increase the computational time.

Motivated by above-mentioned discusses, a novel color image watermarking scheme based on DWT (Discrete Wavelet Transform) and QR decomposition is proposed to embed color watermark image into color host image in this paper. When embedding watermark, the each component of the color host image is transformed by DWT and QR decomposition and all elements in the first row of the matrix R is quantified for embedding the watermark information. Moreover, neither the original host image nor the original watermark image is not needed when extracting watermark. Experimental results show that the proposed color image scheme has stronger robustness against most common attacks such as image compression, filtering, cropping, noise adding etc.

The rest of this paper is organized as follows. QR decomposition is introduced in section 2. The detailed watermark embedding and extraction procedures are presented in section 3. Subsequently, experimental results are given in section 4. Finally, conclusions are made in section 5.

2. Preliminary

2.1 QR Decomposition

In QR decomposition [11], the orthogonal-triangular decomposition of a matrix was performed with the following definition:

$$[Q, R] = qr(A) \tag{1}$$

where R is an $n \times n$ upper triangular matrixand Q is an $n \times n$ unitary matrix, so that $A = Q \times R$. In (1), the columns of Q are obtained from columns of A by Gram-Schmidt orthogonalization process. If we denote A and Q as $A = [a_1, a_2, \cdots, a_n]$, $Q = [q_1, q_2, \cdots, q_n]$, respectively, where a_i and q_i are column vectors, then the matrix R can be computed as:

$$R = \begin{bmatrix} \langle a_1, q_1 \rangle & \langle a_2, q_1 \rangle & \cdots & \langle a_n, q_1 \rangle \\ 0 & \langle a_2, q_2 \rangle & \cdots & \langle a_n, q_2 \rangle \\ \vdots & \vdots & \ddots & \vdots \\ 0 & 0 & 0 & \langle a_n, q_n \rangle \end{bmatrix}$$

where $\langle a_i, q_i \rangle$ is the inner product of a_i and q_i, $i = 1, 2, \cdots, n$.

One of the good properties of R matrix is that when the columns of A have correlation with each other, the absolute values of the elements in the first row of R matrix are probably greater than those in other rows [10]. When the bigger the matrix element in the first row of R matrix is, the bigger the quantization step is, and the bigger the quantization remainder is; if the bigger the quantization remainder is, then the bigger the allowing modification range is.

2.2 Arnold Transform

Arnold transform, which be widely used in image

permutation, is also called Cat Face transfer, and it is given by

$$\begin{pmatrix} x' \\ y' \end{pmatrix} = \begin{pmatrix} a & b \\ c & d \end{pmatrix} \begin{pmatrix} x \\ y \end{pmatrix} (\mathrm{mod}\, N) \tag{2}$$

where a, b, c and d are any positive integers, and $ad - bc = \pm 1$, so only three among the four parameters of a, b, c and d are independent, here, let $a = b = c = 1$, $d = 2$. x', y', x and y are integers in $\{0, 1, 2, \ldots, N-1\}$ and N is order of watermark image matrix. The position (x, y) of watermark image pixel can be changed to another position (x', y') by Eq. (2).

3. The Proposed Watermarking Scheme

In this section, a new double color watermarking scheme is proposed to embed the color image watermark into the R matrix of QR decomposition of color host image. Without loss of generality, let the original host image H be 24-bit color image with size of $M \times M$ and the watermark image be 24-bit color image W with size of $N \times N$. The proposed embedding watermark scheme is illustrated by Figure 1. The detailed embedding procedures are described as follows.

3.1 Watermark Embedding Scheme

Step 1. Pre-processing on color image watermark

Since the color image has much more information than the binary or gray-level image, its binarization process is important because it will directly affect the embedded quality of watermarking. Firstly, 3-D original color watermark image W is divided into three components R, G, B by dimension-reduction treatment. Then, the 2-D component watermarks are obtained corresponding to the R, G and B component, respectively. In order to improve the security of the watermarking, each component watermark is permuted by Arnold transform with private key KA_i (i = 1, 2, 3) and each pixel value is converted to 8-bit binary sequence [12]. Finally, combining all 8-bit binary sequence to form the binary component watermark W_i (i = 1, 2, 3).

Step 2. Block processing of the host image

The host image H is also divided into three components H_i (i = 1, 2, 3), which represent the R, G and B component respectively.

Step 3. Performing DWT

Each component image is transformed by one-level DWT, and low-frequency LL1 part is divided into 4×4 non-overlapping blocks.

Step 4. Performing QR decomposition

Each selected 4×4 block is decomposed by QR decomposition according to Eq. (1) to obtain the upper triangular matrix R.

Step 5. Embedding watermark

The watermark w is embedded by quantifying the first row element of R matrix. The detailed processes are described as follows.

$$r(1,i) = \begin{cases} r(1,i) - \mathrm{mod}(r(1,i), S) + T_1 & if \quad w = '1' \\ r(1,i) - \mathrm{mod}(r(1,i), S) + T_2 & if \quad w = '0' \end{cases} \tag{3}$$

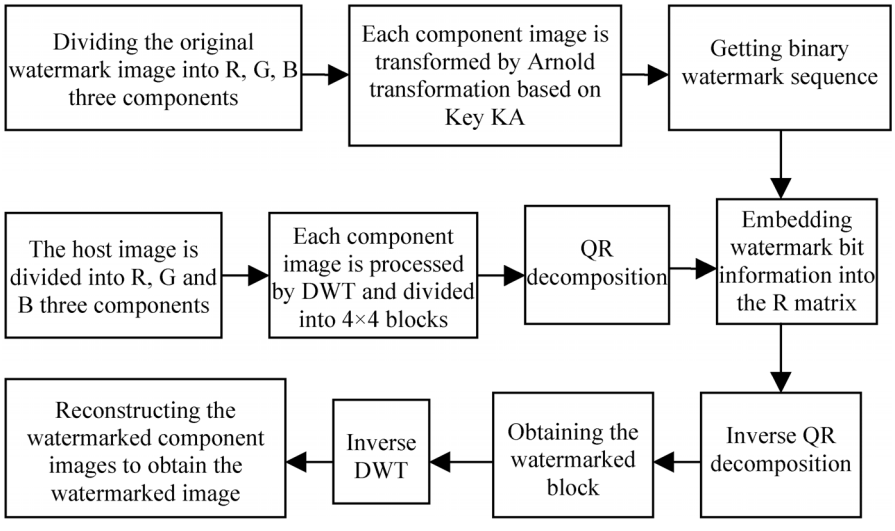

Figure 1. Diagram of the watermark embedding process.

where i is the column number of the first row in the upper triangular matrix R, S is the quantization step, $T_1 = 0.75*S$, $T_2 = 0.25*S$, and mod(.) is the modulo operation.

Step 6. Performing inverse QR operation

When all coefficients in the first row of R matrix, and then apply inverse QR operation to obtain the watermarked image block according to Eq. (4).

$$A' = Q \times R' \tag{4}$$

Step 7. Repetition

Repeat steps 4–6 until all watermark bits are embedded in the DWT low-frequencies of the host image.

Step 8. Inverse DWT

The watermarked R, G, B components are obtained by inverse DWT, and the watermarked image H' is reconstructed by three components.

3.2 Watermark Extraction Scheme

According to whether the original host image and watermark image are needed in the extraction procedure or not, the watermarking scheme could be categorized into blind scheme and non-blind scheme. The proposed watermark extraction procedure, as shown in Figure 2, belongs to blind extraction method, that is, the original host image and watermark image are not needed in the procedure. The detailed steps of the watermark extraction procedure are presented as follows.

Step 1. Pre-processing on the watermarked image

The watermarked image H' is divided into R, G, B component images.

Step 2. Performing DWT

Each watermarked component image is transformed by one-level DWT, and low-frequency LL1 part is divided into 4×4 non-overlapping blocks.

Step 3. Performing QR decomposition

Each watermarked block is decomposed by QR decomposition and its matrix R′ is obtained.

Step 4. Extracting watermark

Each element in the first row of the matrix R' is used to extract the watermark information w′, as shown in Eq. (5).

$$w' = \begin{cases} '0' & if \quad \mathrm{mod}(r(1,i),S) < (T_1 + T_2)/2 \\ '1' & \text{else} \end{cases} \tag{5}$$

where mod(.) is the modulo operation.

Step 5. Repetition

The above steps 2–4 are repeated until all embedded image blocks are performed. These extracted bit values are partitioned into 8-bit groups and converted to decimal pixel values.

Step 6. Reconstruction

Each component watermark is transformed by the inverse Arnold transformation based on the private key KA_i (i = 1, 2, 3). Then, the final extracted watermark W' is reconstructed from the extracted watermarks of the three components.

4. Experimental Results and Discussion

In this paper, the color image of size 32×32 is used as original watermark, as shown in Figure 3, and all 24-bit 512×512 color images in the CVG-UGR image database are used as the host images [13]. Hence, the embedded watermark capacity of this proposed method is (32×32×3×8)/(512×512×3) = 0.03125. For limitation space of the paper, only two 24-bits color images, as shown in Figure 4, are taken for example. By considering the trade off between the robustness and the invisibility of the watermark, let quantization step S = 32.

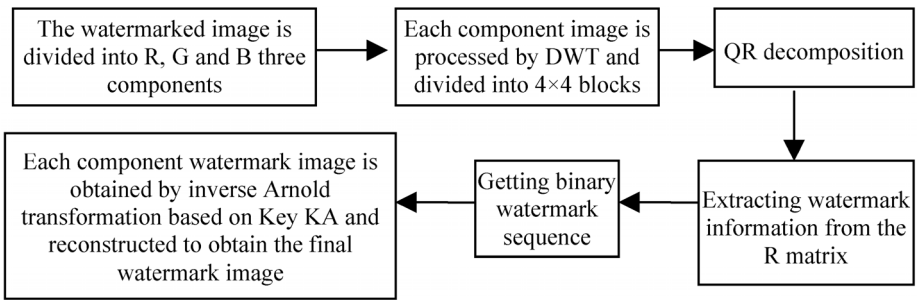

Figure 2. Diagram of the watermark extraction process.

Figure 3. Original watermark image.

(a) (b)

Figure 4. Original host images: (a) Lena, (b) Avion.

The peak signal-to-noise ratio (PSNR) in Eq. (6) is utilized to measure the similarity degree between the original image H and the watermarked image H′.

$$PSNR = 10 \lg \frac{255^2}{MSE} \tag{6}$$

where MSE is the mean square error given by

$$MSE = \frac{1}{3MN} \sum_{j=1}^{3} \sum_{x=1}^{m} \sum_{y=1}^{n} [H(x,y,j) - H'(x,y,j)]^2 \tag{7}$$

where $H(x, y, j)$, $H'(x, y, j)$ present the value of pixel (x, y) in component j of the original image and the watermarked one, and M, N denote the width and height of the host images, respectively.

Moreover, the SSIM developed by Wang et al. [14] was considered to be correlated with the quality perception of the human visual system (HVS). The SSIM, as denoted in Eq. (8), is also used to measure the similarity between the original color image H and the watermarked image H'.

$$SSIM(H,H') = l(H,H')c(H,H')s(H,H') \tag{8}$$

where

$$\begin{cases} l(H,H') = (2\mu_H \mu_{H'} + C_1)/(\mu_H^2 + \mu_{H'}^2 + C_1) \\ c(H,H') = (2\sigma_H \sigma_{H'} + C_2)/(\sigma_H^2 + \sigma_{H'}^2 + C_2) \\ s(H,H') = (\sigma_{HH'} + C_3)/(\sigma_H \sigma_{H'} + C_3) \end{cases} \tag{9}$$

The first term in Eq. (9) is the luminance comparison function which measures the closeness of the two images' mean luminance (μ_H and $\mu_{H'}$). The second term is the contrast comparison function which measures the closeness of the contrast of the two images. Here the contrast is measured by the standard deviation σ_H and $\sigma_{H'}$. The third term is the structure comparison function which measures the correlation coefficient between the two images H and H'. Note that $\sigma_{HH'}$ is the covariance between H and H'. The positive values of the SSIM index are in [0, 1]. A value of 0 means no correlation between images, and 1 means that $H = H'$. The positive constants C_1, C_2 and C_3 are used to avoid a null denominator.

In addition, in order to measure the robustness of the watermark, we use the normalized correlation (NC) between the original watermark W and the extracted watermark W', which isshown as follows.

$$NC = \frac{\sum_{i=1}^{3} \sum_{x=1}^{P} \sum_{y=1}^{Q} (W(x,y,j) \times W'(x,y,j))}{\sqrt{\sum_{j=1}^{3} \sum_{x=1}^{P} \sum_{y=1}^{Q} [W(x,y,j)]^2} \sqrt{\sum_{j=1}^{3} \sum_{x=1}^{P} \sum_{y=1}^{Q} [W'(x,y,j)]^2}} \tag{10}$$

where, P and Q denote the row and column size of the original watermark image.

4.1 Testing the Watermark Invisibility

Generally, a larger PSNR or SSIM indicates that the watermarked image resembles the original host image more closely, which means that the watermarking method makes the watermark more imperceptible. A higher NC reveals that the extracted watermark resembles the original watermark more closely. If a method has a higher NC value when the watermarked image is suffered from an attack, it is more robust.

It can be seen from Figure 5, all embedded watermarks can be completely extracted from the watermarked images without any attacks (all NC values are 1), and the

(a) (b) (c) (d)

Figure 5. Watermarked images: (a) Lena (PSNR = 41.3784 db, SSIM = 0.9879), (b) Avion (PSNR = 41.4141 db, SSIM = 0.9907); Extracted watermark: (c) extracted from (a) (NC = 1), (d) extracted from (b) (NC = 1).

proposed algorithm has better invisibility (its PSNR values are more than 40 db and SSIM values are very bigger). Hence, the proposed method can obtain higher watermark invisibility than other methods.

4.2 Testing the Watermark Robustness

In practice, the watermarked image will be subjected to a variety of distortions before reaching the detector. Watermarks designed to survive legitimate and everyday usage of image, e.g., JPEG compression, noise, filtering, are referred to as robust watermark. To verify the watermark robustness of the proposed method, all watermarked images are attacked by common image processing operations (such as JPEG compression, adding noise, filtering etc.) and geometrical distortions (such as scaling, cropping etc.). In which, the JPEG quality factor is from 10 to 90 with increasing step of 1; JPEG 2000 compression with the compression ratio is from 1 to 10 with increasing step of 1; the noising scheme generates of salt & Peppers noising are 2% and 10% noise; the mean of Gaussian noise parameter are set to 0.1, 0.3; the cut-off frequency of low-pass filtering is 100, and its radius are from 1 to 5; the position of cropping are from upper-left to lower-right; and the watermarked image is scaling from 1/4 to 4 with increasing step of 0.1, respectively. Figure 6 shows the extracted watermarks from the watermarked Lena image by different methods, which verified the robustness of the proposed method. It is noted that the method [10] is only superior to the proposed method in the case of cropping attack, which because the embedding blocks in the method [10] can be randomly selected by the MD5-based Hash pseudo-random replacement algorithm, and the embedding blocks in the proposed method are centralized. In addition, Figure 7(a), (b) gives the NC values of different host images that compared with method [10], respectively. As can be seen from it, the proposed method has better robustness than the method [10] in most cases.

4.3 The Execution Time Comparison of Different Algorithms

In our experiments, a laptop computer with a duo Intel CPU at 2.27 GHZ, 2.00 GB RAM, Win 7, MATLAB 7.10.0 (R2010a) is used as the computing platform. As can be seen from Figure 8, the embedding and extrac-

Attack method	Proposed method		Method [10]	
	Extracted watermark	NC	Extracted watermark	NC
JPEG compression 90		0.99853		0.99617
JPEG 2000 (5:1)		0.99629		0.99175
Salt&Peppers (0.02)		0.99280		0.99209
Gaussian noise (0.1)		0.95951		0.91332
Median filter (3*1)		0.99115		0.76107
Low-pass filter (100,1)		0.98335		0.90489
Croping (0.25)	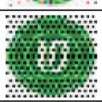	0.73814		0.87722
Scaling (4)		0.99744		0.99123

Figure 6. The comparison of extracted watermark by different methods after different attacks.

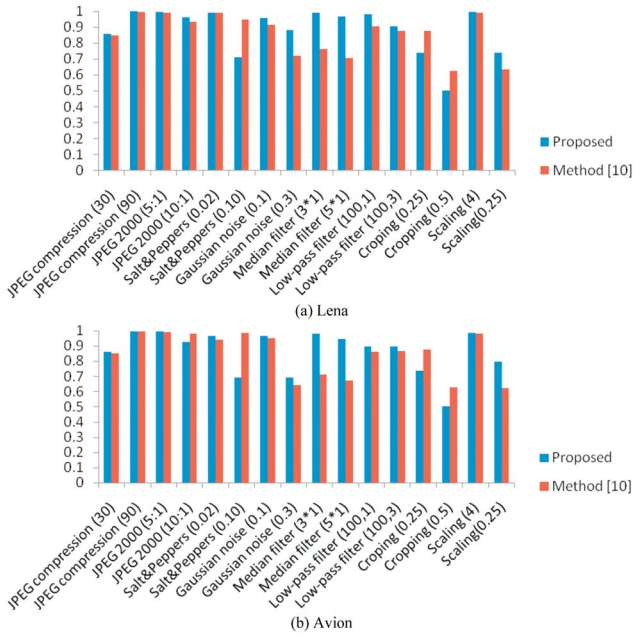

Figure 7. The NC values comparison of extracted watermark from different test images by different methods after different attacks.

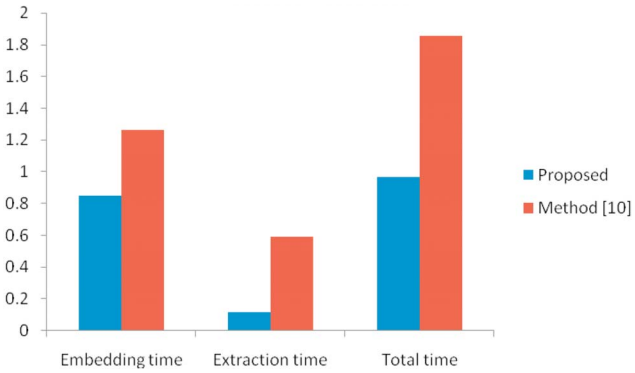

Figure 8. The comparison of execution time between different methods (Second).

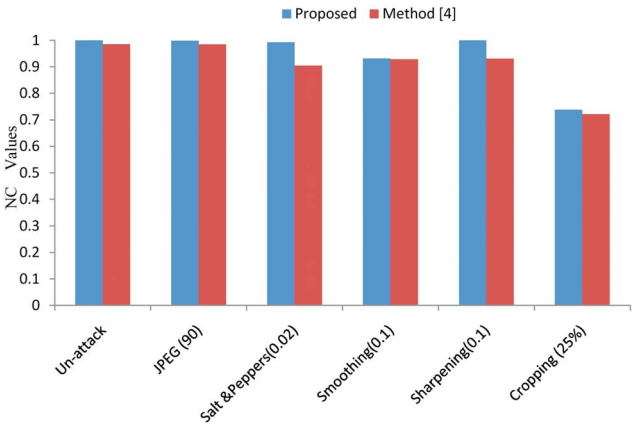

Figure 9. The comparison between the proposed method and the method based on DWT.

tion time of the proposed method is less than that of [10]. That is, the proposed algorithm requires much less number of computations, which because the MD5-based Hash pseudo-random replacement algorithm with private key K_i (i = 1, 2, 3) is used to select the embedding block for embedding watermark in [10].

4.4 The Comparison between the Proposed Method and the Method Based on DWT

In this experiment, our proposed method is also compared with the related method [4] based on DWT. In which, the host image is Lena image and the watermark is shown in Figure 3. For fair comparison, the watermark is extracted from the un-attack image and the attacked images, respectively, and the attack types include JPEG compression (Compression ratio is 90), adding Salt & Peppers noise (noise intensity is 0.02), smoothing (smoothing radius is 0.1), sharpening (sharpening radius is 0.1), and cropping (cropping 25% from upper-left to lower-right). As can be seen from Figure 9, the proposed algorithm has better invisibility (un-attack) and more robust than method [4].

5.Conclusions

In this work, a novel double color algorithm based on DWT and QR decomposition has been proposed. Through using the quantization technique, the color watermark information is embedded into all elements in the first row of the matrix R. Moreover, without resorting to the original host image or original watermark, the embedded watermark can be successfully extracted from the images subject to different attacks. Experimental results have shown that this proposed algorithm not only attains higher invisibility of watermarking, but also has stronger robustness in the operation of common image processing and geometric attacks.

Acknowledgements

The research was partially supported by Natural Science Foundation of Shandong Province (No. ZR2014 FM005), National Science Foundation of China (No. 61502218, 61572258), Shandong Province Important Research Plan Projects (No. 2015GSF116001), Key Sci-

ence and Technology Plan Projects of Yantai City (No. 2016ZH057), Taishan Scholars Talent Project of Shandong Province (No. tshw201502050), and Outstanding Young Scientists Foundation Grant of Shandong Province (No. BS2014DX016). The authors would like to thank anonymous referees for their valuable comments and suggestions which lead to substantial improvements of this paper.

References

[1] Li, X. W. and Kim, S. T., "An Improved Cellular Automata-based Digital Image Watermarking Scheme Combining the Use of Pixel-wise Masking and 3D Integral Imaging," *Optics Communications*, Vol. 319, No. 5, pp. 45–55 (2014). doi: 10.1016/j.optcom.2013.12.089

[2] An, L., Gao, X., Li, X., Tao, D., Deng, C. and Li, J., "Robust Reversible Watermarking via Clustering and Enhanced Pixel-wise Masking," *IEEE Transactions on Image Processing*, Vol. 21, No. 8, pp. 3598–3611 (2012). doi: 10.1109/TIP.2012.2191564

[3] Su, Q., Niu, Y., Zou, H. and Liu, X., "A Blind Dual Color Images Watermarking Based on Singular Value Decomposition," *Applied Mathematics and Computation*, Vol. 219, No. 16, pp. 8455–8466 (2013.) doi: 10.1016/j.amc.2013.03.013

[4] Ming, S. H. and Chang, T. D., "Wavelet-based Color Image Watermarking Using Adaptive Entropy Casting," Proceedings of the IEEE International Conference on Multimedia and Expo, pp. 1593–1596 (2006). doi: 10.1109/ICME.2006.262850

[5] Golea, N. E. H., Seghir, R. and Benzid, R., "A Bind RGB Color Image Watermarking Based on Singular Value Decomposition," 2010 IEEE/ACS International Conference on Computer Systems and Applications (AICCSA), pp. 1–5 (2010). doi: 10.1109/AICCSA.2010.5586967

[6] Li, X. H. and Fan, H., "QR Factorization Based Blind Channel Identification and Equalization with Second-order Statistics," *IEEE Transaction on Signal Processing*, Vol. 48, No. 1, pp. 60–69 (2000). doi: 10.1109/78.815479

[7] Moor, B. D. and Dooren, P. V., "Generalizations of the Singular Value and QR Decompositions," *SIAM Journal on Matrix Analysis and Applications*, Vol. 13, No. 4, pp. 993–1014 (1992). doi: 10.1137/0613060

[8] Yashar, N. and Saied, H. K., "Fast Watermarking Based on QR Decomposition in Wavelet Domain," 2010 Sixth International Conference on Intelligent Information Hiding and Multimedia Signal Processing, pp. 127–130 (2010). doi: 10.1109/IIHMSP.2010.39

[9] Song, W., Hou, J., Li, Z. and Huang, L., "Chaotic System and QR Factorization Based Robust Digital Image Watermarking Algorithm," *Journal of Central South University of Technology*, Vol. 18, No. 1, pp. 116–124 (2011). doi: 10.1007/s11771-011-0668-8

[10] Su, Q., Niu, Y., Wang, G., Jia, S. and Yue, J.,"Color Image Blind Watermarking Scheme Based on QR Decomposition," *Signal Processing*, Vol. 94, No. 1, pp. 219–235 (2014). doi: 10.1016/j.sigpro.2013.06.025

[11] Ahn, C. J., "Parallel Detection Algorithm Using Multiple QR Decompositions with Permuted Channel Matrix for SDM/OFDM," *IEEE Transactions on Vehicular Technology*, Vol. 57, No. 4, pp. 2578–2582 (2008). doi: 10.1109/TVT.2007.913179

[12] Chen, W., Quan, C. and Tay, C. J., "Optical Color Image Encryption Based on Arnold Transform and Interference Method," *Optics Communications*, Vol. 282, No. 18, pp. 3680–3685 (2009). doi: 10.1016/j.optcom.2009.06.014

[13] University of Granada, Computer Vision Group. CVG-UGR Image Database. [2012-10-22]. http://decsai.ugr.es/cvg/dbimagenes/c512.php

[14] Wang, Z., Bovik, A. C., Sheikh, H. R. and Simoncelli, E. P., "Image Quality Assessment: from Error Visibility to Structural Similarity," *IEEE Transactions on Image Processing*, Vol. 13, No. 4, pp. 600–612 (2004). doi: 10.1109/TIP.2003.819861

Manuscript Received: Jul. 4, 2016
Accepted: Jan. 12, 2017